GOLD NANOPARTICLES

1. Introduction

Nanoparticles have become important materials in modern technologies compared with their bulk analogues not only as a result of their excellent structural features but also as a result of their unusual functional attributes. Most of the bulk materials we use in everyday life such as steel or sand are composed of micrometer scale particles. The properties of a material are related to the bonding/interactions acting between and within its constituent units. Scientists are discovering new ways to reduce the size of constituent particles of every material to the nanometer length scale (to produce nanomaterials) as it gives them one way to modify the properties of materials. Besides reduction in size, controlling chemical composition at such smaller length scales also can result in new properties. Advances in nanofabrication and synthesis provided new ways to manipulate the size of materials. In gold, the changes in size of constituent particles to nanometer scale result in drastic modification of its properties. Such changes in dimension can be realized even with simple chemical manipulations, and such modified gold is extremely stable allowing diverse phenomena to be examined. Therefore, gold has been a material of choice for nanoscience enthusiasts. Importantly, these changes can be examined with the simplest of tools available in any laboratory that took GNP research to every nook and corner of the world. Gold has been an object fascinating to knowledge-seekers since prehistoric times, and applications of GNPs have grabbed the attention of researchers in the information age. Systematic efforts in the synthesis and evaluation of properties of GNPs have exposed new avenues to some very unique and exciting capabilities. Although this article provides an outline of the present understanding of GNPs, as a result of space constraints, it will only briefly touch on the historical aspects and theoretical understanding of the optical and spectroscopic properties. For more detailed information, we direct the readers to several books and review articles (1–14).

2. Historical Perspective of Gold Nanoparticles

Gold nanoparticles have a rich history in chemistry, dating back to ancient Roman times, where GNPs were used to stain glasses with intense shades of different colors (13,15,16). More than 5000 years ago, the Egyptians used gold for mental, bodily, and spiritual purification (17). Several civilizations used gold in medicinal preparations. The system of medicine called Ayurveda uses preparations, *Saraswatharishtam* and *Makaradwajam*, containing gold used for internal applications. Medieval artisans (400 to 1300 AD) have used a mixture of gold salts with molten glass to produce tiny gold colloids with a rich ruby color, and its variations were exploited for coloration of glass, ceramics, china ware, and pottery. One of the most fascinating examples is the Lycurgus Cup that was made in the fourth century AD and a sample of which is kept in the British Museum in London (Fig. 1). The Lycurgus Cup features an amazing property of changing color depending on the way light fell on it. In reflected light, it appears green, whereas it is ruby red in transmitted light (Fig. 1). Later study

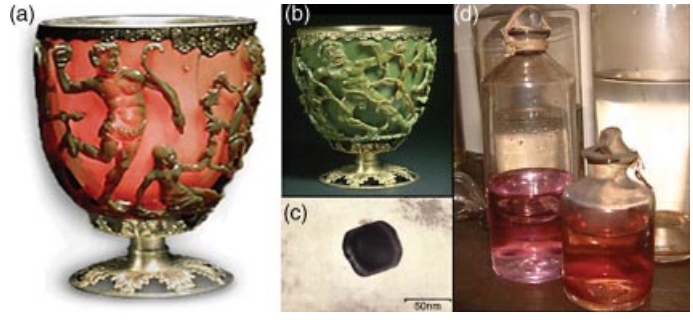

Fig. 1. (**a** and **b**) The Lycurgus Cup made from glass appears red in transmitted light and green in reflected light (adapted from Ref. 24). The cup alone is the creation of fourth century AD, and the metallic holder is a later addition. (**c**) The 70-nm Au-Ag alloy nanoparticles found in the glass of the Lycurgus Cup as seen in the transmission electron micrograph (adapted from Ref. 24). (**d**) Faraday's gold preserved in the Royal Institution (25).

on this revealed that this optical phenomenon is a result of the presence of mixed Au–Ag particles of approximately 70 nm diameter within the glass matrix.

In the seventeenth century, the medicinal values of colloidal gold were well used for curing various diseases, such as heart and venereal problems, dysentery, epilepsy, and tumors. It was also used for diagnosis of syphilis. In the eighteenth century, many philosophers have identified the curative properties of a drinkable and slightly pink colloidal gold solution. Of course, the reason behind the optical and other unusual properties of colloidal gold was totally unknown at that time. The next major step in the development of nanotechnology happened in 1857, when Michael Faraday reported for the first time the formation of deep, red-colored colloidal gold (Fig. 1**d**) by reduction of an aqueous solution of chloroaurate ($AuCl_4^-$) using phosphorus in CS_2 (18). He found that colloidal gold had special optical and electrical properties. From the twentieth century onward, various methods for the preparation of gold colloids were reported (19–23).

3. General Synthetic Strategies

The strategies used belong to two classes, top-down and bottom-up, just as in other nanomaterials. Top-down refers to synthesis starting from bulk materials by reducing their size, and bottom-up refers to creating larger structures by building from the small, ie, starting from atoms.

3.1. Citrate Reduction Method. The citrate reduction method was developed by J. Turkevich and co-workers in 1951 (26). This method is the most popular one and is considered the conventional method of synthesis of GNPs. In this method, sodium citrate usually acts as both the reducing and the stabilizing agent (although other reducing agents, such as amino acids, have also been successfully used) and is reacted with Au^{3+} at elevated temperatures making colloidal suspensions. This method can result in reasonably monodisperse spherical GNPs of size around 10–20 nm in diameter. The particle size can be increased by reducing the amount of sodium citrate. This method was

modified by Frens in 1973 to obtain GNPs of predetermined size via their controlled formation, where the trisodium-citrate-to-gold ratio was varied (27). Although many papers refer to these dispersions as *solutions*, they are true *colloids* that scatter visible light, and this can be observed by passing a beam of laser (as in a laser pointer) through it.

3.2. The Brust–Schiffrin Method. Brust and Schiffrin developed a method in 1994 for making thermally stable and monodisperse GNPs of size ranging between 1.5 and 5.2 nm via a facile synthetic procedure (28). The Brust method involves phase transfer of Au^{3+} from the aqueous phase to the organic phase by a phase-transfer reagent, tetraoctyl ammonium bromide, and their subsequent reduction at the interface by the reducing agent, $NaBH_4$, in the presence of a thiol to form thiolate (RS—) protected GNPs. The size of the nanoparticles can be varied by changing the Au:thiol ratio. These GNPs can be repeatedly isolated and redissolved in organic solvents without irreversible aggregation or decomposition. Functionalization of these particles can be carried out by synthesis using functionalized thiols or by the ligand exchange process. Such GNPs are also called monolayer protected clusters (MPCs) as the ligands protecting the gold surface are similar to self-assembled monolayers (SAMs), which is an active area of research. Using this approach, it is also possible to synthesize several water-soluble MPCs from various water-soluble thiols such as glutathione and mercaptosuccinic acid.

3.3. Seed-mediated Growth Method. The seed-mediated method is a modified form of Zsigmondy's "nuclear" method (29) to make nanoparticles via a two-step process. However, the "seeding" method to make bigger colloidal Au nanoparticles of size 30–100 nm was first demonstrated by Brown and Natan (30). Later, Murphy and co-workers introduced the seed-mediated growth approach to make nanoparticles of various shapes (31,32). Anisotropic noble metal nanoparticles of various shapes such as rods (33), wires (34), triangles (35), stars (36), flowers (37,38), and so on can be conveniently synthesized using this method. The seeding-growth procedure is a two-step process wherein the "seed nanoparticles" synthesized in the first step will be converted into nanoparticles of other shapes in the second step in the presence of a "growth solution." The growth solution contains excess metal ions, a surfactant or shaping agent, and a mild reducing agent. In this process, the surfactant molecules will form suitable templates that facilitate the growth process to yield nanoparticles of desired morphology. The seed need not always be a metal nanoparticle. The metal salts will get reduced on the surface of the seed nanoparticles and grow into nanoparticles of desired shapes in the second step of this process. The size of the nanoparticles can also be tuned by changing the amount of seed nanoparticles added.

3.4. Biological Synthesis. Biological synthesis is considered a safe and eco-friendly method to make GNPs as this method involves the use of organisms ranging from bacteria to fungi, various parts of plants, and biological extracts (14, 39–42). This method yields the nanoparticles of improved biocompatibility capable of many biomedical applications because the as-synthesized nanomaterials are decorated/protected with biological species. Using this method, GNPs of various shapes such as triangles, wires, spheres, plates, and so on (14,43,44) have been synthesized. A high percentage of thin, flat,

single-crystalline gold nanotriangles have been synthesized at room temperature by the reduction of aqueous chloroaurate ions ($AuCl_4^-$) by lemongrass (*Cymbopogon flexuosus*) extract (45). The reducing sugars (aldoses) present in the lemongrass extract were found to reduce Au^{3+} into nanoprisms. Apart from this, extracts of tamarind leaf (46), *Cinnamomum zeylanicum* leaf (47), unicellular green algae, and *Chlorella vulgaris* (48) have been used to produce various GNPs.

3.5. Electrochemical Synthesis. The electrochemical method was first proposed by Reetz and Helbig in 1994 (49). They showed that highly size-selective nanoparticles can be made by the electrochemical reduction method by adjusting the current density. This method can be used for making diverse GNPs such as cubes, rods, triangles, plates, and so on (50). This method has many advantages over other methods because it has a lower processing temperature, lower cost, requires modest equipment, and offers good control of size, shape, and morphology. A high yield of suspended gold nanorods has been synthesized by this method by using a two-electrode setup (51). In this process, a gold metal plate and a platinum plate are used as anode and cathode, respectively. These electrodes were immersed in an electrolytic solution consisting of a cationic surfactant or stabilizing agent, and a co-surfactant. During this process, the bulk gold metal is oxidized at the anode and the metal cations reduce at the interfacial region of the cathodic surface to form gold nanorods in the presence of the stabilizing agent. GNPs of various aspect ratios can be synthesized by this method.

3.6. Other Methods. It has been found that gold ions can be reduced via radiolytic (52) and photochemical (53,54) methods. GNPs of various morphologies such as rods, triangles, plates, and hexagons can be generated using the photochemical method (53,54). Template-assisted (55) methods have been used to make one-dimensional nanostructures with uniform size and controllable physical dimensions. In this process, nanoporous polycarbonate or alumina is used as a template. The method is based on the electrochemical deposition of metals in the template structure. Galvanic displacement reaction (56) is another method to make GNPs and its hybrid forms. This is a single-step method that works based on the differences in the standard electrode potentials of various elements, leading to deposition of the more noble element and dissolution of the less noble element (57,58). Many other techniques such as sonolysis (59), microwave-assisted synthesis (60,61), and the hydrothermal method (62) are being used to make GNPs. All above-mentioned methods come under the category of the bottom-up approach of synthesizing nanoparticles.

GNPs can also be synthesized via top-down routes. Nanosphere lithography (63) is a powerful technique to produce nanoparticle arrays with controlled shape, size, and interparticle spacing, which uses self-assembled polystyrene nanospheres as templates. Using this method, different nanostructures such as triangles, disks, chains, rings, and so on have been generated successfully (63). Dip-pen nanolithography (64) is a new AFM-based, soft-lithography technique being used to generate layers on Au, combined with wet-chemical etching to fabricate various nanostructures such as lines, dots, rings, and triangles. Other top-down techniques such as photolithography and electron beam lithography (65) have also been used to make GNPs. As nanoparticles produced by

top-down approaches follow expensive synthetic pathways that are industrially nonscalable, bottom-up approaches are far more popular in the synthesis of nanoparticles.

4. Properties of Gold Nanoparticles

As the physical and chemical properties of nanoparticles depend on the spatial confinement of electrons, the properties of GNPs vary depending on their size, shape, degree of aggregation, and local environment. GNPs show unusual optical properties that are different from their bulk analogue. They show characteristic colors depending on the size, shape, and dielectric constant of the surrounding medium. Spherical GNPs have a characteristic wine red color. This is a result of its localized surface plasmon resonance (LSPR) (8,66). Because of the poor penetration power of electromagnetic waves on a metal surface, the plasmon excitations are caused only by surface electrons when materials are irradiated with low energy radiations. These excitations are referred to as surface plasmons in the case of metals. Figure 2**a** shows such a plasmon, which causes alternating positive and negative charges that propagate in the x- and y-directions along the metal-dielectric interface, and decay momentarily in the z-direction. When an electromagnetic radiation of an appropriate wavelength interacts with a gold nanostructure, the conduction electrons near a metal-dielectric interface get excited and undergo a collective oscillation relative to the lattice of positive

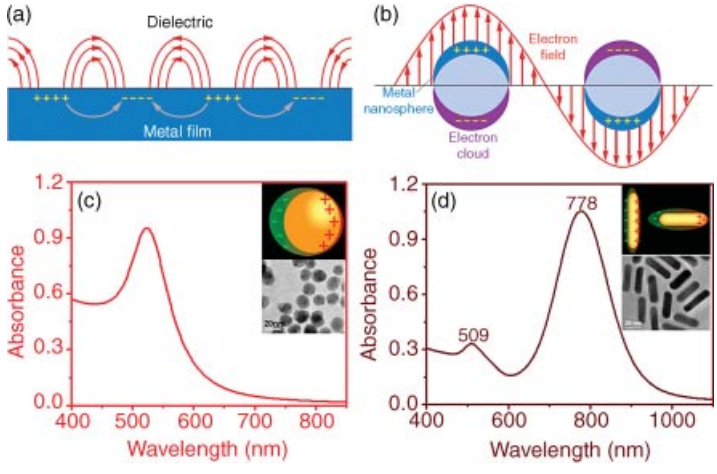

Fig. 2. (**a**) Excitation of surface plasmon on metal film causes alternating positive and negative charges that propagate in the x- and y-directions along the metal-dielectric interface. (**b**) Localized surface plasmons in metal nanospheres (adapted from Ref. 66). **c** and **d** are extinction spectra of gold nanospheres and nanorods, respectively. Corresponding TEM images of spherical and rod-shaped GNPs are shown in the inset. The insets of **c** and **d** also show the schematic illustrations of polarization of the conduction electrons with respect to the ionic core in the case of spherical and rod-shaped nanoparticles. The polarized electron cloud is shown in green, and the metal particle is shown in orange.

nuclei at the frequency of the incoming light. In the case of metal nanoparticles, collective oscillation of free electrons is confined to a finite volume; hence, the corresponding plasmon is called a localized surface plasmon. The electric field of the incident wave can cause free electrons to move away from the metal particle in the field direction. This can create a dipole that can switch direction with the change in electric field (Fig. 2**b**). These oscillations can result in the generation of a momentary electric field over the metal surface, which can be extended into the dielectric over a nanometer length scale. This enhanced field is several orders of magnitude above the incident field, which brings about novel properties for the particles.

Investigations into the interaction between gold colloids and light were begun by Faraday, in the nineteenth century. In 1908 Gustav Mie developed a complete theory for the scattering and absorption of the electromagnetic radiation by spheres, in order to understand the plasmon resonance absorption and color of gold colloids in solution (67). This is called the Mie theory and is applicable to only spherical particles. According to Mie theory, the total extinction cross section comprises contributions from both the scattering and absorption cross sections; ie, the extinction cross section, $\sigma_{\text{ext}} = \sigma_{\text{abs}} + \sigma_{\text{scat}}$ (absorption cross section + scattering cross section). For nanoparticles that are much smaller than the wavelength of light ($\lambda \gg 2\text{r}$, where r = radius of the nanoparticles), the Mie theory reduces to (68–70)

$$\sigma_{\text{ext}}(\omega) = 9\frac{\omega}{c}\varepsilon_{\text{m}}^{3/2}V\frac{\varepsilon_2(\omega)}{\left[\varepsilon_1(\omega) + 2\varepsilon_{\text{m}}\right]^2 + \varepsilon_2(\omega)^2}$$

where V is the volume of the particle [$(4\pi/3)\text{r}^3$], ω is the angular frequency of the exciting light, c is the velocity of light, ε_{m} is the dielectric function of the surrounding medium of the nanoparticles, and $\varepsilon_1$and $\varepsilon_2$are the real and imaginary parts of the dielectric function of the nanoparticles, respectively; ie, $\varepsilon(\omega) = \varepsilon_1(\omega) + i\varepsilon_2(\omega)$. The resonance occurs when $\varepsilon_1(\omega) = -2\varepsilon_{\text{m}}$, if ε_2 is small and is a weekly dependent function of ω. The resonance will happen around $\lambda = 520$ nm for gold in air (71). In 1912, Gans extended Mie theory to both oblate and prolate spheroidal particles and predicted two well-defined, distinct surface plasmon modes for spheroidal metal nanoparticles (72).

The LSPR of gold nanostructures depends on several variables, particularly the size, shape, electron density, effective mass, dielectric function, and its environment. Gold nanorod is a better example to demonstrate the shape-dependent LSPR properties. The optical spectrum of gold nanorods does not show only one well-defined resonance peak as in the case of nanospheres. It exhibits two bands in the visible–near-infrared (NIR) spectral range (Fig. 2**d**). Theoretical studies suggest that the band near 530 nm is a result of transverse LSPR, which is polarized across (corresponding to electron oscillation perpendicular to) the long axis of the nanorod, and the other one, appearing at a longer wavelength, has been assigned to a longitudinal LSPR mode, which is polarized along (parallel to) the long axis (Fig. 2). For other anisotropic nanoparticles such as disks, stars, and triangular prisms, the LSPRs are typically split into distinctive dipole and quadrupole plasmon modes (73). The higher order multipole plasmon resonances

such as quadrupole and octapole modes become important as the nanoparticle becomes larger and anisotropic. The excitation of such higher order modes can be attributed to the inhomogenous polarization of the nanoparticles by the electromagnetic field as the particle size becomes comparable with the wavelength of the incoming radiation (74).

Surface plasmon resonance can result in huge enhancement in the local electric field around the GNP surfaces (75,76). When an electromagnetic field excites the free electrons at the of a tip of a GNP or a rough metallic surface, a highly localized and strong electric field develops at these sharp tips or vertices enhancing the Raman scattering cross section about several orders of magnitude (as Raman scattering intensity is proportional to the fourth power of the electric field) (77,78). This so-called surface enhanced Raman scattering (SERS) is an effect observed in 1974 by Fleischman and co-workers (79), which enables single-molecule Raman spectroscopy. The SERS activity mainly depends on factors such as size and shape of the nanoparticles, dielectric environment, wavelength of the excitation light source, and interparticle spacing between the nanoparticles (80). For example, gold mesoflowers (38) and triangles (35) are observed to have higher SERS activity than its spherical analogue, as a result of the higher electric field generated at the tips and edges of these nanoparticles. The plasmonic properties of the GNPs can be modulated through the deposition of a dielectric material onto them. It has been found that silica-coated GNPs can enhance the sensitivity of SERS substrates and that even detection of adsorbed hydrogen is possible with such materials (81). Recently, hybrid gold nanomaterials have been shown to exhibit remarkable new physical properties such as surface-plasmon–based lasing (82) and light-controlled manipulation of spin (83). Mulvaney's and Liz-Marzan's papers on oxide-protected GNPs showed new possibilities for such materials in plasmonic applications (73,84,85). It is shown that the silica-coated gold nanorods can amplify the photoacoustic response without altering the optical absorption of nanoparticles (86). Such materials can be used as contrast agents for more sensitive photoacoustic imaging.

GNPs comprise hundreds to several thousands of gold atoms. They have an electronic structure that contains aspects of both the discrete energy levels as in atoms or molecules and the band structure seen in metals. When the size of the GNPs reduces to <2 nm, they lose their metallic character substantially and start exhibiting molecular transitions under ambient conditions. Because very small GNPs (<2 nm) do not possess the continuous band structure like bulk gold, they will have intriguing electronic properties that make them useful for many applications in the area of nanoelectronics. Although gold is inert in bulk, GNPs show very good catalytic activity. In 1987, M. Haruta and co-workers found that GNPs of less than 10 nm have a high degree of catalytic activity when they are deposited on metal oxide supports (87). They are very effective in converting toxic carbon monoxide into carbon dioxide at room temperature. As a result of the nontoxic nature and high surface-to-volume ratio, GNPs are highly attractive as catalysts for a variety of chemical reactions such as hydrogenation, CO oxidation, selective oxidation, and nucleophilic additions (88,89). Hybrid GNPs have unique properties, and they will be discussed in the section titled "Hybrid Gold Nanoparticles."

5. Anisotropic Gold Nanoparticles

Anisotropic nanomaterials are a class of materials that show direction and dimension-dependent physical and chemical properties (50). Anisotropic GNPs have been attractive to scientists for the past few decades as a result of their biocompatibility, unique physical and chemical properties, as well as promising applications in diverse areas such as sensing, catalysis, bioimaging, photothermal therapy, targeted drug delivery, nanoelectronics, photonic and plasmonic devices, and so on (50). Particle anisotropy offers unique features and functions that are difficult to obtain for isotropic nanoparticles. A variety of chemical methods (see the synthesis section) have been developed to fabricate a diverse spectrum of anisotropic GNPs (Fig. 3) such as nanorods, nanowires, nanotubes, triangles, plates, sheets, ribbon, pyramids, stars, flowers, multi-pods, urchins, tadpole, cages, rice, boxes, cubes, triangular nanoframes, and so on (50,90,91). As a result of the widespread applications in many areas, gold nanorods and triangles have received significant attention, and many reliable and well-established methods have been developed to make them in high yield and monodispersity. The optical properties of anisotropic GNPs are tunable throughout the visible, NIR, and infrared (IR) regions of the spectrum, as a function of their aspect ratios. This is prominent in the case of gold nanorods and prisms. Even though spherical GNPs show intense LSPR absorption with a good absorption coefficient, the strength of absorption is weakly dependent on its size, which limits its application in sensing. When anisotropy is added to the nanoparticles, such as nanorods or prisms, the LSPR is not only enhanced but also becomes strongly tunable with their aspect ratio. Generally, increasing the number of edges, highly active crystallographic facets, corners, and faces tends to exhibit improved catalytic performance in such particles (88).

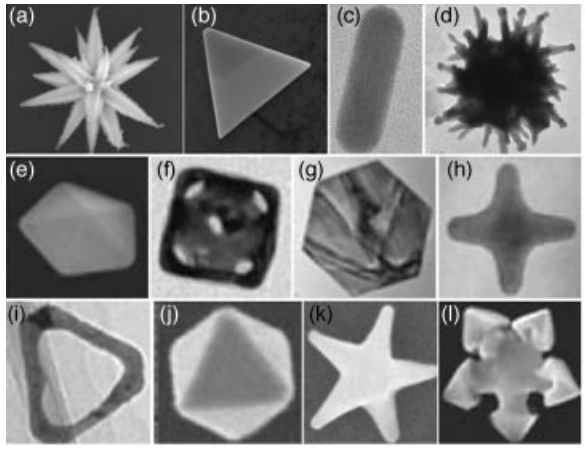

	Gold nanostructures	Ref.
a	Flower	38
b	Triangle	77
c	Rod	91
d	Meat-ball	38
e	Decahedron	100
f	Cage	100
g	Hexagon	100
h	Tetrapode	100
i	Ring	100
j	Octahedron	100
k	Star	100
l	Snowflake	100

Fig. 3. Microscopic images of various anisotropic GNPs. References from which the images are taken are indicated in the table. The particles occur in the size range of 30 nm to 10 μm.

In many synthetic procedures, shape control of GNPs has been achieved by suitably controlling the experimental parameters such as concentration of the metal precursor, reducing agents and stabilizers, and the reaction conditions such as temperature and time. In certain cases, formation of surfactant micelles, structural defects, and anisotropic interactions of different crystal facets with surfactants and solvents would physically direct the anisotropic growth of the GNPs. The energetic aspects can also play an important role in determining the anisotropic growth of the nanoparticles. However, it remains a great challenge to elucidate fully the exact role of these parameters in determining the morphology of the nanoparticles. At the same time, it has been proposed that the synergistic effect of various experimental parameters has substantial influence on the final shape of the nanoparticle.

6. Hybrid Gold Nanoparticles

Incorporating additional functionalities into nanoscale objects is one way to tailor their physical and chemical properties. Hybrid nanoparticles belong to an important class of nanomaterials because they exhibit multifunctional properties arising as a result of the effective coupling of different metal domains (92) and because they find applications in diverse areas. For example, the LSPR of the various domains in a hybrid system can interact in interesting ways, and it can be enhanced, shifted, or suppressed. Core-shell and alloy GNPs exhibit enhanced physical and chemical properties compared with their monometallic analogues (81,92). A hybrid nanoparticle made by the incorporation of fluorescence and magnetic attributes would be naturally more advantageous. The luminescence property makes the nanoparticles suitable for bio-detection and bio-sensing, and the magnetic attribute makes them promising for targeted drug delivery, magnetic bio-separation, and detection. The hybrid systems of GNPs with biological moieties have helped solve several technical difficulties in medical and biosciences (7,37,56). For example, antibody–nanoparticle hybrid systems can be used for the detection of antigens (7). The emergence of new properties is identified in many hybrid materials made of gold such as nanorice (93), nanocages (56), nanocobes (94), triangular nanoframes (95), mesoflowers (96–98), and so on. It is also possible to tune the optical and catalytic properties of hybrid gold nanomaterials within a single nanostructure (92,99).

7. Assembled Gold Nanostructures

Fabrication of various nanoparticles into their one-, two-, or three-dimensional assembled structures brings novel properties to the resulting system as a result of the effective coupling of different domains. GNPs and their self-assemblies have been investigated extensively as a result of their biocompatibility, tunable optical properties, and easiness in synthesis. Such self-assembled superstructures are useful in studying specific properties such as SERS, metal-insulator transition, and inter-plasmon coupling.

GNPs can be arranged over various templates such as DNA (100,101), carbon nanotubes (102), polymers (103), and so on. The unique molecular recognition capability and structural features of DNA have been exploited to program the assembly of GNPs (Fig. 4). A more recent development in this direction is the DNA-origami strategy (100), which can be used to engineer almost any arbitrary pattern. Using DNA as a template, GNPs have been arranged to form nanoparticles molecules, and various one-, two-, or three-dimensional nanoparticle crystals (Fig. 4) (100). Brust and co-workers have shown that assemblies of GNPs can be made using bifunctional dithiol links (104). Here, each thiol molecule present in the linker molecule can attach to two nanoparticles. Rao and Kalyanikutty have demonstrated the assembly of GNPs at liquid–liquid interfaces (105).

Well-defined one-, two-, or three-dimensional GNPs can be arranged with molecular linkers, templates, or spacers into regular periodic two- or three-dimensional assembled structures called particle crystals or superlattices (Fig. 4) (106–110). Such self-assembled superstructures can be achieved by bottom-up or top-down approaches. The most important requirement to make superlattices is to have monodisperse particles that can order over a long

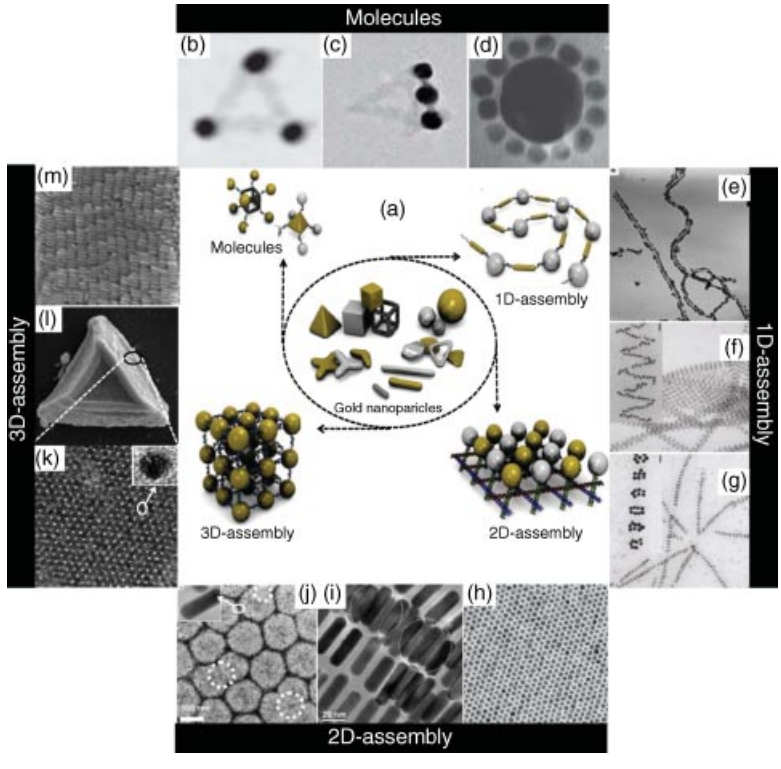

Fig. 4. (**a**) Schematics of various assemblies from constituting nanoparticles (adapted from Ref. 100; image has been modified from the original figure). **b**–**d** (adapted from Ref. 100), **e**–**g** (adapted from Refs. 100 and 102), **h**–**j** (adapted from Refs. 100,90, and 103), and **k**–**m** (adapted from Refs. 113 and 114) are molecular, one-, two-, and three-dimensional assemblies, respectively, made of various GNPs. **k** is an expanded TEM image of a portion of superlattice shown in **l**.

range. The collective properties of individual nanoparticles in superlattice can help to understand charge transport properties such as metal-insulator transitions and changes in optical properties such as inter-plasmon coupling. (106). Recently, Pradeep and co-workers have demonstrated that GNP superlattices can be used as a SERS substrate and also they can be used as functional solids for concomitant conductivity and SERS tuning (108–111). Superlattices of GNPs can be formed by electrostatic self-assembly, solvent evaporation on substrates, self-organization at interfaces, covalent and hydrogen bonding, biochemical interactions, as well as van der Waals and dipole interactions (112).

Superlattices of gold have been synthesized by digestive ripening and by the solvated metal atom dispersion method (SMAD) and hydrogen bonding method (112). Highly monodispersed thiol-protected spherical GNPs synthesized by the solvated metal SMAD method followed by digestive ripening have a great tendency to self-organize into two- and three-dimensional nanocrystal superlattices. The successful organization of mercaptosuccinic acid protected GNPs into beautiful three-dimensional structures in solution can be made by the addition of an acid (pH $\sim$ 2) to the nanoparticle dispersions (107,111). Here, the self-assembly happens as a result of hydrogen bonding. The superlattice forms a brown mirror-like appearance at the air/water interface after a few days (113). During the crystal formation, particles produce different morphologies.

Many anisotropic GNPs can also organize to make assembled structures (Fig. 4) (114). The added advantage of anisotropic nanoparticle assembly is that the same nanomaterial can interact and assemble in different ways as a result of its inherent anisotropy in the structure, which will result in novel properties. In the case of gold nanorods, depending on the functionalizing molecule, the assembly can be formed through a wide variety of operating forces such as covalent, hydrogen bonding, electrostatic, biochemical interaction, van der Waals and dipole interactions, and so on (6,50). As a result of the anisotropic crystal structure and difference in surface reactivity, gold nanorods can be selectively functionalized to bring forth specific interactions between the constituent nanostructures resulting in their end-to-end or side-by-side assembly. Because gold nanorods are covered by CTAB, a stabilizing bilayer, the suspension gets stabilized devoid of any tendency to aggregate as a result of the electrostatic repulsion between the head groups of CTAB on adjacent rods (115). But, when the excess surfactant is removed by centrifugation and the conditions like concentration, pH, and ionic strength are optimum, there can be a situation where the electrostatic repulsion is being compensated by the hydrophobic–hydrophobic interaction between the CTAB tails. This will facilitate the assembly of NRs. Highly organized superlattices of Au nanorods with plasmonic antenna enhancement of an electrical field have been used for fast and direct detection of prions in complex biological media such as serum and blood (116).

8. Supported Gold Nanoparticles

Immobilization of metal nanoparticles on a suitable high-surface-area solid helps to reduce the mobility of the metal nanoparticles to diminish their tendency to agglomerate. Apart from this, the chemical reactivity of nanoparticles can

be significantly altered by the nature of the support. The characteristics of the support such as surface area, porosity, presence of surface hydroxyl groups, surface defects, and crystal structure influence the adsorption ability of the support. GNPs supported on active carbons with a high surface area have been widely used as catalysts for hydrogenations and oxidations. Other than active carbon, oxides such as Al_2O_3, SiO_2, MgO, TiO_2, MnO_2, and their mixed oxides can also be used as good supports for heterogeneous catalysis (117). There are numerous methods available to attach nanoparticles on supports (117). One of the easiest methods for the immobilization of GNPs on the support is the impregnation method. It is also possible to make supported nanoparticles by the adsorption technique. Deposition–precipitation is an alternative to the adsorption technique to obtain supported GNPs on metal oxides.

Supported GNPs have been widely used for the removal of severely toxic contaminants such as pesticides, halogenated organics, heavy metals, and micro-organisms from drinking water (117–120). For making a nanoparticles-based water purifier, it is important that the nanoparticles are anchored on suitable substrates and they are not easily removed from the support during use. As a result of this reason, highly dispersed nanoparticles on supports such as oxides, fibers, and polymers are used for water purification. GNPs have the capacity to adsorb reasonable quantities of hydrogen and oxygen on its surface; hence, it plays an important role in the hydrogenation or oxidation reactions of organic compounds. A remarkable change in the catalytic activity can be observed in supported GNPs (eg, catalytic oxidation of CO). It has been shown that 3-nm GNPs attached on supports such as TiO_2, Fe_2O_3, and Co_2O_3 are very active for CO oxidation compared with other conventional supports like SiO_2 and Al_2O_3, on which they are practically inactive. The reason for this was interpreted in terms of the formation of an active GNPs–metal-oxide interface along the perimeter of GNPs (13). The poor catalytic activity of TiO_2 nanoparticles on visible light irradiation can be overcome by doping them with GNPs. An enhanced photocatalytic activity is reported for Au/TiO_2nanoparticles (121,122). This system has been used for various applications such as hydrogen generation, dye decoloration, phenol decomposition, carboxylic acid degradation, and so on (121,123). Many GNPs-based catalysts are being developed for industrial applications (124). GNPs alloyed with other precious metals have been used in the automotive industry as catalytic convertors to reduce harmful emissions from the engine exhaust (124).

9. Applications of Gold Nanoparticles

The unique properties exhibited by GNPs such as surface plasmon resonance, SERS, nonlinear optical properties, and quantized charging effect have been used for a variety of applications in the areas of biolabeling, bioimaging, sensors, catalysis, nanodevices, nanoelectronics, and so on (13,32,125–127). Some of the important applications of GNPs are mentioned in this section.

9.1. Biological Applications. *Bioimaging.* Although gold has a long history as a material for many therapeutic applications, the advancement that took place in the area of nanochemistry broadened its potential in various

biomedical applications. Apart from the biocompatibility, the unique properties, and easiness in functionalization with various biological molecules, GNPs have been used for targeting and to deliver a therapeutic dose of drugs into cancer cells. The large extinction cross sections and tunable optical absorption of GNPs such as nanorods, nanotriangles, and nanocages in the near-infrared region (the wavelength region where blood and tissues are relatively transparent to the radiation) enables them to be good candidates for diagnosis and in many other medical applications. The strong surface plasmon resonance of metal nanoparticles enables one to image an individual particle location with various optical microscopic techniques such as dark-field optical and two-photon luminescence microscopy (128). Gold nanorods and nanocages are ideal candidates for cancer cell imaging as a result of its tunable SPR peaks and scattering in the near-infrared. The utility of gold nanocages as an optical contrasting agent has been demonstrated by optical coherence tomography imaging (56). Gold nanoshells are a new class of nanoparticles developed by Halas and co-workers, which show strong absorption and scattering of light in the NIR region, capable of many biological applications (129). GNPs have been widely used for various biosensing strategies (130,131).

Photothermal Therapy. Nanoparticles of gold are the perfect raw material for robust and rapid diagnostic testing as well as for many therapeutic applications. Living cells are highly sensitive to the temperature, and a rise of a few degrees can lead to cell death. The near-infrared absorption and related photothermal effect is another important feature of anisotropic GNPs (56,125). Compared with the other nonmetallic photothermal absorbers, the GNPs enable dual-imaging/therapy functions. It has been demonstrated with several anisotropic nanomaterials, such as nanorods, nanotriangles, nanocages, and nanostars, that they can be used for the photothermal therapy (56,125).

9.2. Surface-enhanced Raman Scattering. GNPs have received considerable attention as a result of their high SERS (76) activity and have a significant advantage in trace detection of molecules. They are found to be useful for many applications in trace analysis of pesticides, biomolecules, bacteria, virus, specific antigens, glucose, explosive materials, and so on (132). Single-molecule detection is possible using SERS, and several protein and nucleic acid biosensors have been designed using this property of GNPs (132). Mirkin and co-workers showed that GNPs functionalized with oligonucleotides and Raman labels, coupled with SERS, can be used to perform multiplexed detection of RNA and DNA (132). Gold mesoflowers are a new class of materials that show good SERS activity (38,98).

9.3. Sensors. The properties of GNPs such as intense surface plasmon resonance and scattering of visible light have been also used for sensing applications. A variety of GNP-based LSPR sensing schemes have been developed for organic vapors (134). A composite material made of GNPs with pH-sensitive polymers have been used in a variety of pH sensing schemes. Conjugates of GNPs-oligonucleotides showed their significant role in precise detection of DNA sequences. Mirkin and co-workers have demonstrated a new colorimetric technique based on the sensitivity of the LSPR band of the GNPs to monitor DNA modifications. Using GNPs, Geddes and co-workers have developed a LSPR-based glucose sensor (135). Haick and co-workers showed that an array

of sensors based on GNPs can rapidly distinguish the breath of lung cancer patients from the breath of healthy individuals (136). Advances in nanotechnology have led to the development of a GNP-based bio-barcode amplification assay, to detect an HIV-1 p24 antigen at very low concentrations (137).

9.4. Water Purification. *Metal Ion Sensing.* GNP-based technologies are showing great promise in providing solutions to several environmentally important issues. They are highly promising for sensing and removal of heavy metal ions from water (119,120,138). GNPs-based colorimetric sensors have been widely used in this direction, which can overcome some of the limitations of conventional methods because these assays do not use organic solvents, light-sensitive dye molecules, and sophisticated instrumentations. By analyzing the shift in the intensity and absorbance maximum of the LSPR band of the nanoparticles, it is possible to detect various heavy metal ions such as Hg, Pb, Cd, and so on. Recently, a facile, cost-effective, and sensitive colorimetric detection method for Pb^{2+} has been developed by using glutathione functionalized GNPs (139). Gold nanorods are capable for quick and selective sensing of mercury in tap water samples at the ppt level (140). The selectivity and sensitivity of mercury are a result of the amalgamation of mercury and gold.

Removal of Water Contaminants. GNPs have also been shown to be efficient adsorbents for removing significant quantities of mercury from water. Complete removal of mercury from water can be done at room temperature by using GNPs supported on alumina (118). By monitoring the shift in their LSPR, enhanced visual detection of pesticides in ppb level is possible by using GNPs (141). One other important breakthrough in water treatment technologies is the development of catalytically active bimetallic gold-palladium nanoparticles for the degradation of various chlorinated hydrocarbons, such as trichloroethane (142). Pradeep and co-workers have demonstrated that GNPs can be used for the detection and removal of many organochlorine and organophosphorus pesticides effectively from drinking water (118,141,143,144).

9.5. Catalysis. Catalysis with active oxide-supported GNPs is now an expanding area, and several new catalytic systems for various reactions have been widely exploited for many applications. GNPs can oxidize highly toxic CO to a far less toxic carbon dioxide (87). More recent investigations have shown that GNPs adsorbed and dispersed on oxide support can be used as efficient catalysts for hydrogenation of unsaturated substrates (13). Thus, shape and crystal structure differences can lead to different catalytic rates (145). In homogeneous catalysis, Narayanan and El-Sayed demonstrated that nanoparticles with more corners and edge atoms have a higher reactivity than similar nanoparticles with fewer corner and edge atoms (145,146).

9.6. Other Applications. GNPs are also used in solar cells to improve the efficiency as the GNPs enhance the optical absorption in the range of visible light (13). It has been recognized that near-infrared absorbing films made by GNPs can be used as an alternative to reflective coatings for blocking IR radiation. Using a prototypical device, Pradeep and Sajanlal have demonstrated that NIR-IR absorption exhibited by gold mesoflowers can absorb a significant amount of heat, thereby reducing the temperature rise in an enclosure exposed to daylight (38). Murray and co-workers have demonstrated that a single redox reaction taking place at the surface of Au nanocrystals induces an eightfold

increase in its capacitance (147). Schiffrin and co-workers have introduced a nano-switch based on a layer of GNPs on a viologen moiety anchored to a gold substrate (148). GNPs improve the efficiency of a rechargeable battery. It was found that the efficiency of rechargeable lithium-air batteries can be enhanced significantly by using a gold/platinum alloy nanoparticle as a catalyst, which will be useful in making high-energy-density batteries practical for use in electric vehicles (149). Nanoscale gold coating on standard graphite anodes can enhance the efficiency of microbial electrochemical cells more than standard palladium coatings, which may find promising applications in sewage treatment (150). GNPs have been used as an active ingredient in cosmetics.

Knowledge about the potential toxicity and health impact of nanoparticles is essential before their large-scale use. The cellular toxicity of GNPs with regard to particle size, shape, and surface group has been extensively investigated by many research groups (32,151,152). Jahnen-Dechen and co-workers have demonstrated that gold particles of size 1–2 nm are highly toxic in nature and that larger 15-nm gold colloids are comparatively nontoxic (153). At the same time, Rotello and co-workers found that cationic GNPs are moderately toxic, whereas anionic GNPs are nontoxic (152). However, several studies have been suggesting that the observed cytotoxicity of GNPs can be reduced by making an overcoating with various materials such as poly(ethyleneglycol), phosphatidylcholine, and polyelectrolytes (154–156).

10. New Materials of Gold—Quantum Clusters

Quantum clusters (QCs) are a new class of materials made up of a few tens of atoms, below 1 nm in core size, which exhibit unusual physical and chemical properties as a result of their molecule-like nature (157,158). QCs act as a bridge between molecular and nanoparticle behaviors, and they possess entirely different properties from both of these size regimes. They possess an intermediate chemical composition between bulk and molecular regimes, where their electronic band structure gets modified into discrete electronic states as a result of quantum confinement. QCs exhibit strong and core size-dependent, tunable photoluminescence properties. They show characteristic absorption features, and they are photo-stable too. The quantum yield of gold QCs is several times higher than that of bulk gold. The photoluminescence property, photo-stability, and biocompatiblity exhibited by the gold QCs makes them potential for many biorelated applications such as labeling, cell imaging, drug delivery, detection, and so on (157).

Monolayer protected gold QCs can be synthesized by various methods (157,159). They can be directly synthesized from the precursor ions where these ions (Au^{3+}) are reduced by a reducing agent (e.g., $NaBH_4$) in the presence of stabilizing ligands such as thiols, amino acids, proteins, dendrimers, and so on (158). Quantum clusters can also be made inside cavities. Red luminescent Au_{15} QCs were synthesized inside cyclodextrin cavities by partial encapsulation (160). Luminescent gold QCs have been embedded also in silica shells (161). A series of glutathione-capped gold QCs have been synthesized by reducing gold ions in the presence of glutathione, followed by their separation using the polyacrylamidegel

electrophoresis (PAGE) method. A new QC can be made from another QC by treating it with appropriate ligands. QCs are also synthesized by core etching processes (159). In this process, core etching of NPs using appropriate ligands like dendrimers and thiols or Au^{3+} ions results in the formation of QCs (162). Gold clusters are also highly stable at ambient conditions.

In the case of gold QCs, the electronic bands will resolve into discrete energy levels that resemble that of the organic molecules. Hence, they can be treated as molecular entities. For example, Au_{25} shows multiple molecular-like transitions in its optical spectrum (163). The luminescence quantum yield of gold QCs synthesized ranges approximately from 70% to 0.1%. Although the mechanism of luminescence in QCs is not fully known exactly, it is believed that the emission originates from radiative intraband transitions within the sp bands, across the HOMO–LUMO gap. As the size of the cluster decreases, the spacing between the discrete states increases; this leads to a blue shift in the emission of smaller QCs as compared with their larger analogues. Pradeep and co-workers has demonstrated that fluorescence resonance energy transfer (FRET) can take place between the metal core and ligands in gold quantum clusters (164,165).

Because the QCs are biocompatible and luminescent, they are promising candidates for bio-related applications such as targeted imaging of cancer cells, biolabeling, drug delivery, and so on (157,165). These clusters can be easily conjugated with biological molecules, which further enhance their application potential. For example, Au_{23} quantum clusters have been used to image human hepatoma (HepG2) cell lines by avidin–biotin interaction (166). Gold QCs can also be used for renal clearance. An ideal nanomaterial-based contrast agent should be effectively cleared out from the body without accumulation in organs. *In vivo* applications using noble metal nanoparticles are severely hampered by their slow renal clearance and high, nonspecific accumulation in the organs. Recently, it was found that the glutathione-coated luminescent gold nanoclusters can be used for renal clearance with a better efficiency than GNPs (167). Most of the metal QCs emit in the NIR region, and hence, they can be used for two-photon imaging with IR excitation (159). Two-photon emission of Au_{25} is observed at 830 nm by exciting at 1290 nm, and this can be used for two-photon imaging with IR excitation (157). QCs also exhibit electroluminescence at room temperature and hence provide facile routes to produce strong single-photon emitters (157). Luminescence of gold QC is exploited for metal ion sensing (166). Fluorescent gold QCs can be used to sense mercury (II) based on fluorescence quenching through Hg(II)-induced aggregation (168). Quantum clusters are very good catalysts (157,169,170). As the crystal structures of QCs are known, it is possible to correlate the particle structure with catalytic properties (171,172). It was found that the metal oxide (e.g., Fe_2O_3, TiO_2) supported gold QCs show higher catalytic activity and yield compared with unsupported QCs (157).

11. Advanced Technologies

Advances in the field of nanoscience and nanotechnology have widened the potential of gold, and many companies have emerged to focus the capabilities

of GNPs. The world Gold Council plays a pivotal role in the development of GNP-based technologies in diverse areas of energy, environment, and medicine. Since 1980, more than 5600 tons of gold have been used in the electronic and electrical industries. CytImmune is a clinical stage nanomedicine company focused on the discovery, development, and commercialization of multifunctional, tumor-targeted therapies. Recently, in a phase 1 clinical trial, scientists from CytImmune have demonstrated that a unique nanomedicine that uses GNPs can be used for tumor-targeted drug delivery (173). Another company called Nanospectra has conducted successful early phase human trials on treatments for solid tumors based on gold nanotechnology. Gold-based technologies are also being used by many pharmaceutical companies. A GNP-based, unique, needle-free delivery system has developed by a company called PowerMed. A U.K.-based company, Premier Chemicals supplies GNPs catalysts supported on carbon under the name of NanAucat. A U.S company, Nanostellar, commercialized the first GNP-based catalytic converter for automobile exhausts. GNP-based pregnancy kits are now commercially available in the market. A pregnancy testing kit that was marketed by Church and Dwight uses GNPs bound to a specific DNA sequence that is sensitive to the presence of a hormone indicative of pregnancy. Numerous other companies and academic groups are in the process of commercializing gold-based products for many applications.

12. Future Directions

As the research in nanotechnology is growing rapidly, many of the unusual properties of the GNPs will be used for making ultrasmall and ultrafast devices for many electronic and bio-related applications. The properties of many GNPs are studied only to a limited extent. Although there are many promising avenues in terms of their medical and materials science applications, more work is needed to bring these into reality. Development of new instrumental techniques capable of manipulating individual nanomaterials and of visualizing their functions may lead to new and exciting possibilities of "nano surgery," wherein site-specific cell or gene therapy can be done. In this way, genetic defects could be identified and rectified even before birth. Multifunctional and stimuli-responsive GNPs with programmable functions would be useful for targeting and killing harmful bacteria and viruses that are likely to penetrate into the body. The strong near-infrared absorbing property of gold nanomaterials can be used to produce highly promising optical filters. Since the properties of GNPs and clusters are extremely sensitive to their size and shape, precise computational methods capable of providing more information about the crystal structures and response of nanoparticles would be desirable for developing new sensing devices. Understanding the crystal structures of such noble metal quantum clusters can give new insight into their extraordinary catalytic activity and other properties. New quantum clusters-based catalysts may develop in the near future that can overcome the limitations of many conventional catalysts. Novel photophysical properties and high catalytic activity of gold quantum clusters would make them a promising candidate in artificial photosynthesis. The extremely small size and high luminescence of gold quantum clusters can help monitor fundamental life processes

such as replication of DNA and genomic changes. The development of hybrid and multimodal gold quantum clusters can be used as smart material with improved efficiency in medical diagnosis and therapy. Recent research and understanding on the use of various GNPs in cancer diagnostics and therapy has already set the platform for the development of clinical applications in the near future. In this direction, the unique properties of gold nanoshells suggest a promising future in biology. More precise kinetic theory is yet to develop, which can predict not only the evolution of a single nanoparticle, but also provide an insight into the influence of various parameters on the growth of nanoparticles under a range of conditions. In parallel, the study of the cytotoxicity of nanoparticles as a function of its size, shape, and surface coating may find much attention in the future.

BIBLIOGRAPHY

1. C. Corti and R. Holliday, *Gold: Science and Applications*, CRC Press, Boca Raton, Fla., 2009.
2. P. E. Chow, *Gold Nanoparticles: Properties, Characterization and Fabrication*, Nova Science Publishers, Inc., Hauppauge, N.Y., 2010.
3. M. Haruta, *Gold Nanotechnology: Fundamentals and Applications*, Shi Emu Shi Shuppan Co., Ltd., Tokyo, Japan, 2009.
4. F. Mohr, *Gold Chemistry: Applications and Future Directions in the Life Sciences*, Wiley-VCH Verlag GmbH & Co. KGaA, Weinheim, Germany, 2009.
5. X. Huang, S. Neretina, and M. A. El-Sayed, *Adv. Mater.* **21**, 4880–4910 (2009).
6. V. Sharma, K. Park, and M. Srinivasarao, *Mater. Sci. Eng. R: Rep.* **65**, 1–38 (2009).
7. N. L. Rosi and C. A. Mirkin, *Chem. Rev.* **105**, 1547–1562 (2005).
8. P. K. Jain and co-workers, *Acc. Chem. Res.* **41**, 1578–1586 (2008).
9. S. Eustis and M. A. El-Sayed, *Chem. Soc. Rev.* **35**, 209–217 (2006).
10. M. Chen and D. W. Goodman, *Acc. Chem. Res.* **39**, 739–746 (2006).
11. M. Grzelczak and co-workers, *Chem. Soc. Rev.* **37**, 1783–1791 (2008).
12. V. Myroshnychenko and co-workers, *Chem. Soc. Rev.* **37**, 1792–1805 (2008).
13. M.-C. Daniel and D. Astruc, *Chem. Rev.* **104**, 293–346 (2003).
14. C. Burda, *J. Am. Chem. Soc.* **131**, 6642 (2009).
15. A. S. Marfunin, *History of Gold*, Nauka, Moscow, Russia, 1987.
16. G. Morteani and J. P. Northover, *Prehistoric Gold in Europe: Mines, Metallurgy and Manufacture. (Proceedings of the NATO Advanced Research Workshop on Prehistoric Gold in Europe, Seeon, Germany, September 27-October 1, 1993.) [In: NATO ASI Ser., Ser. E, 1995; 280]*, Kluwer Academic Publishers, Boston, Mass., 1995.
17. A. Moores and F. Goettmann, *New J. Chem.* **30**, 1121–1132 (2006).
18. M. Faraday, *Philos. Trans. R. Soc. London, Ser.* **147**, 145–181 (1857).
19. G. W. Hacker and J. Gu, *Gold and Silver Staining: Techniques in Molecular Morphology*, CRC Press, Boca Raton, Fla., 2002.
20. M. A. Hayat, *Colloidal Gold: Principles, Methods, and Applications*, Vol. 3, Academic Press, Inc., Orlando, Fla., 1991.
21. V. Cabral and R. Silva, *Nanomaterials: Properties, Preparation and Processes*, Nova Science Publishers, Inc., Hauppauge, N.Y., 2010.
22. A. S. Edelstein and R. C. Cammarata, *Nanomaterials: Synthesis, Properties and Applications*, Institute of Physics, Bristol, Penn., 1996.
23. C. N. R. Rao, A. Mueller and A. K. Cheetham, *Nanomaterials Chemistry: Recent Developments and New Directions*, Wiley-VCH Verlag GmbH & Co. KGaA, Weinheim, Germany, 2007.

24. www.thebritishmuseum.ac.uk
25. www.rigb.org/rimain/heritage/faradaypage.jsp
26. J. Turkevich, P. C. Stevenson, and J. Hillier, *Discuss. Faraday Soc.* **11**, 55–75 (1951).
27. G. Frens, *Nature Phys. Sci.* **241**, 20–22 (1973).
28. M. Brust and co-workers, *J. Chem. Soc., Chem. Commun.*, 801–802 (1994).
29. R. Gans, *Ann. Phys.* **47**, 270–284 (1915).
30. K. R. Brown and M. J. Natan, *Langmuir* **14**, 726–728 (1998).
31. N. R. Jana, L. Gearheart, and C. J. Murphy, *Adv. Mater.* **13**, 1389–1393 (2001).
32. C. J. Murphy and co-workers, *Acc. Chem. Res.* **41**, 1721–1730 (2008).
33. B. D. Busbee, S. O. Obare, and C. J. Murphy, *Adv. Mater.* **15**, 414–416 (2003).
34. X. Lu and co-workers, *J. Am. Chem. Soc.* **130**, 8900–8901 (2008).
35. P. R. Sajanlal and T. Pradeep, *Adv. Mater.* **20**, 980–983 (2008).
36. F. Hao and co-workers, *Nano Lett.* **7**, 729–732 (2007).
37. Z. Wang and co-workers, *Nano Lett.* **10**, 1886–1891 (2010).
38. P. R. Sajanlal and T. Pradeep, *Nano Res.* **2**, 306–320 (2009).
39. P. Mukherjee and co-workers, *Angew. Chem., Int. Ed.* **40**, 3585–3588 (2001).
40. J. L. Gardea-Torresdey and co-workers, *Nano Lett.* **2**, 397–401 (2002).
41. J. Xie and co-workers, *Small* **3**, 672–682 (2007).
42. B. Nair and T. Pradeep, *Cryst. Growth Des.* **2**, 293–298 (2002).
43. J. G. Parsons, J. R. Peralta-Videa, and J. L. Gardea-Torresdey, *Dev. Environ. Sci.* **5**, 463–485 (2007).
44. C. S. Han, H. Y. Lee, and Y. Roh, *Int. J. Nanotechnol.* **3**, 236–252 (2006).
45. S. S. Shankar and co-workers, *Nat. Mater.* **3**, 482–488 (2004).
46. B. Ankamwar, M. Chaudhary, and M. Sastry, *Synth. React. Inorg. Met.-Org. Chem.* **35**, 19–26 (2005).
47. S. L. Smitha, D. Philip, and K. G. Gopchandran, *Spectrochim. Acta, Part A* **74**, 735–739 (2009).
48. M. Hosea and co-workers, *Inorg. Chim. Acta* **123**, 161–165 (1986).
49. M. T. Reetz and W. Helbig, *J. Am. Chem. Soc.* **116**, 7401–7402 (1994).
50. P. R. Sajanlal and co-workers, *Nano Rev.* **2**, 5883 (2011).
51. Y.-Y. Yu and co-workers, *J. Phys. Chem. B* **101**, 6661–6664 (1997).
52. K. Dick and co-workers, *J. Am. Chem. Soc.* **124**, 2312–2317 (2002).
53. S. Eustis, H.-Y. Hsu, and M. A. El-Sayed, *J. Phys. Chem. B* **109**, 4811–4815 (2005).
54. F. Kim, J. H. Song, and P. Yang, *J. Am. Chem. Soc.* **124**, 14316–14317 (2002).
55. M. R. Jones and co-workers, *Chem. Rev.* **111**, 3736–3827 (2011).
56. S. E. Skrabalak and co-workers, *Acc. Chem. Res.* **41**, 1587–1595 (2008).
57. B. Wiley and co-workers, *MRS Bull.* **30**, 356–361 (2005).
58. K. An and T. Hyeon, *Nano Today* **4**, 359–373 (2009).
59. C.-H. Su, P.-L. Wu, and C.-S. Yeh, *J. Phys. Chem. B* **107**, 14240–14243 (2003).
60. Y.-J. Zhu and X.-l. Hu, *Chem. Lett.* **32**, 1140–1141 (2003).
61. S. Horikoshi and co-workers, *Nanoscale* **3**, 1697–1702 (2011).
62. C.-C. Chang and co-workers, *Chem. Mater.* **20**, 7570–7574 (2008).
63. J. P. Camden and co-workers, *Acc. Chem. Res.* **41**, 1653–1661 (2008).
64. K. Salaita, Y. Wang, and C. A. Mirkin, *Nat. Nano.* **2**, 145–155 (2007).
65. G. M. Wallraff and W. D. Hinsberg, *Chem. Rev.* **99**, 1801–1822 (1999).
66. X. Lu and co-workers, *Annu. Rev. Phys. Chem.* **60**, 167–192 (2009).
67. G. Mie, *Ann. Phys.* **25**, 377 (1908).
68. E. Hutter and J. H. Fendler, *Adv.Mater.* **16**, 1685–1706 (2004).
69. U. Kreibig and M. Vollmer, *Optical Properties of Metal Clusters*, Vol. 25, Springer-Verlag, Berlin, Germany, 1995.
70. S. Link and M. A. El-Sayed, *Int. Rev. Phys. Chem.* **19**, 409–453 (2000).
71. S. Link and M. A. El-Sayed, *J. Phys. Chem. B* **103**, 4212–4217 (1999).

72. R. Gans, *Ann. Phys.* **342**, 881 (1912).
73. J. Nelayah and co-workers, *Nat. Phys.* **3**, 348–353 (2007).
74. K.-Z. Kouroush and F. Benjamin, *Nanotechnology-enabled Sensors*, Springer, New York, 2008.
75. K. A. Willets and D. R. P. Van, *Annu. Rev. Phys. Chem.* **58**, 267–297 (2007).
76. G. C. Schatz, *Acc. Chem. Res.* **17**, 370–376 (1984).
77. P. R. Sajanlal and co-workers, *J. Mater. Chem.* **20**, 2108 (2010).
78. J. Zhao and co-workers, *Acc. Chem. Res.* **41**, 1710–1720 (2008).
79. M. Fleischmann, P. J. Hendra, and A. J. McQuillan, *Chem. Phys. Lett.* **26**, 163–166 (1974).
80. M. D. Porter and co-workers, *Chem. Soc. Rev.* **37**, 1001–1011 (2008).
81. J. F. Li and co-workers, *Nature* **464**, 392–395 (2010).
82. M. A. Noginov and co-workers, *Nature* **460**, 1110–1112 (2009).
83. J. Zhang and co-workers, *Nature* **466**, 91–95 (2010).
84. L. M. Liz-Marzan, M. Giersig, and P. Mulvaney, *Langmuir* **12**, 4329–4335 (1996).
85. I. Pastoriza-Santos and co-workers, *Phys. Chem. Chem. Phys.* **6**, 5056–5060 (2004).
86. Y.-S. Chen and co-workers, *Nano Lett.* **11**, 348–354 (2011).
87. M. Haruta and co-workers, *Chem. Lett.* 405–408 (1987).
88. J. Xiao and L. Qi, *Nanoscale* **3**, 1383–1396 (2011).
89. O. Vaughan, *Nat. Nanotechnol.* **5**, 5–7 (2010).
90. P. R. Sajanlal and co-workers, *Langmuir* **24**, 4607–4614 (2008).
91. T. Sreeprasad, A. Samal, and T. Pradeep, *Bull. Mater. Sci.* **31**, 219–224 (2008).
92. M. B. Cortie and A. M. McDonagh, *Chem. Rev.* **111**, 3713–3735 (2011).
93. H. Wang and co-workers, *Acc. Chem. Res.* **40**, 53–62 (2007).
94. R. Gunawidjaja and co-workers, *Adv. Mater.* **20**, 1544–1549 (2008).
95. G. S. Metraux and co-workers, *Nano Lett.* **3**, 519–522 (2003).
96. P. R. Sajanlal and T. Pradeep, *J. Phys. Chem. C* **114**, 16051–16059 (2010).
97. P. R. Sajanlal and T. Pradeep, *Langmuir* **26**, 456–465 (2010).
98. P. R. Sajanlal and T. Pradeep, *Langmuir* **26**, 8901–8907 (2010).
99. M. Schrinner and co-workers, *Adv. Mater.* **20**, 1928–1933 (2008).
100. S. J. Tan and co-workers, *Nat. Nanotechnol.* **6**, 268–276 (2011).
101. S. Y. Park and co-workers, *Nature* **451**, 553–556 (2008).
102. M. A. Correa-Duarte and co-workers, *Angew. Chem., Int. Ed.* **44**, 4375–4378 (2005).
103. V. R. R. Kumar and co-workers, *Langmuir* **23**, 8667–8669 (2007).
104. M. Brust and co-workers, *Adv. Mater.* **7**, 795–797 (1995).
105. C. N. R. Rao and K. P. Kalyanikutty, *Acc. Chem. Res.* **41**, 489–499 (2008).
106. K. Kimura and T. Pradeep, *Phys. Chem. Chem. Phys.* **13**, 19214–19225 (2011).
107. N. Nishida and co-workers, *Adv. Mater.* **20**, 4719–4723 (2008).
108. E. S. Shibu, K. Kimura, and T. Pradeep, *Chem. Mater.* **21**, 3773–3781 (2009).
109. C. P. Collier, T. Vossmeyer, and J. R. Heath, *Annu. Rev. Phys. Chem.* **49**, 371–404 (1998).
110. N. Sandhyarani and T. Pradeep, *Int. Rev. Phys. Chem.* **22**, 221–262 (2003).
111. E. S. Shibu and co-workers, *Nanoscale* **3**, 1066–1072 (2011).
112. B. L. V. Prasad, C. M. Sorensen, and K. J. Klabunde, *Chem. Soc. Rev.* **37**, 1871–1883 (2008).
113. E. S. Shibu and co-workers, *Nano Res.* **2**, 220–234 (2009).
114. A. Guerrero-Martínez and co-workers, *Angew. Chem., Int. Ed.* **48**, 9484–9488 (2009).
115. T. S. Sreeprasad, A. K. Samal, and T. Pradeep, *Langmuir* **24**, 4589–4599 (2008).
116. R. A. Alvarez-Puebla and co-workers, *Proc. Natl. Acad. Sci. U.S.A.* **108**, 8157–8161 (2011).
117. T. Pradeep and Anshup, *Thin Solid Films* **517**, 6441–6478 (2009).
118. K. P. Lisha, Anshup, and T. Pradeep, *Gold Bull.* **42**, 144–152 (2009).

119. A. Sreekumaran Nair and T. Pradeep, Indian Pat. 200767 (2006).
120. A. Sreekumaran Nair and T. Pradeep, U.S. Pat. 7,968,493B2 (2011).
121. A. Primo, A. Corma, and H. Garcia, *Phys. Chem. Chem. Phys.* **13**, 886–910 (2011).
122. H. Tada, T. Kiyonaga, and S.-i. Naya, *Chem. Soc. Rev.* **38**, 1849–1858 (2009).
123. P. V. Kamat, *J. Phys. Chem. C* **111**, 2834–2860 (2007).
124. S. A. C. Carabineiro and co-workers, *Catalytic Applications for Gold Nanotechnology Nanocatalysis*, Springer, Berlin, Germany, 2007.
125. P. K. Jain and co-workers, *Acc. Chem. Res.* **41**, 1578–1586 (2008).
126. R. A. Sperling and co-workers, *Chem. Soc. Rev.* **37**, 1896–1908 (2008).
127. R. Philip and co-workers, *Phys. Rev. B* **62**, 13160 (2000).
128. H. Wang and co-workers, *Proc. Natl. Acad. Sci. U.S.A.* **102**, 15752–15756 (2005).
129. S. Lal, S. E. Clare, and N. J. Halas, *Acc. Chem. Res.* **41**, 1842–1851 (2008).
130. U. H. F. Bunz and V. M. Rotello, *Angew. Chem., Int. Ed.* **49**, 3268–3279 (2010).
131. Y. Xiao and co-workers, *Science* **299**, 1877–1881 (2003).
132. M. J. Banholzer and co-workers, *Chem. Soc. Rev.* **37**, 885–897 (2008).
133. Y. C. Cao, R. Jin, and C. A. Mirkin, *Science* **297**, 1536–1540 (2002).
134. K. M. Mayer and J. H. Hafner, *Chem. Rev.* **111**, 3828–3857 (2011).
135. K. Aslan, J. R. Lakowicz, and C. D. Geddes, *Anal. Chem.* **77**, 2007–2014 (2005).
136. G. Peng and co-workers, *Nat. Nano.* **4**, 669–673 (2009).
137. S. Tang and co-workers, *J. Acqui. Imm. Def. Syns.* **46**, 231–237 (2007).
138. G. Aragay, J. Pons, and A. Merkoci, *Chem. Rev.* **111**, 3433–3458 (2011).
139. F. Chai and co-workers, *ACS Appl. Mater. Interfaces* **2**, 1466–1470 (2010).
140. M. Rex, F. E. Hernandez, and A. D. Campiglia, *Anal. Chem.* **78**, 445–451 (2005).
141. K. P. Lisha, Anshup, and T. Pradeep, *J. Environ. Sci. Health., Part B* **44**, 697–705 (2009).
142. K. N. Heck and co-workers, *J. Catal.* **267**, 97–104 (2009).
143. A. Sreekumaran Nair, R. T. Tom, and T. Pradeep, *J. Environ. Monit.* **5**, 363–365 (2003).
144. A. S. Nair and T. Pradeep, *J. Nanosci. Nanotechnol.* **7**, 1871–1877 (2007).
145. S. Eustis and M. A. El-Sayed, *Chem. Soc. Rev.* **35**, 209–217 (2006).
146. R. Narayanan and M. A. El-Sayed, *J. Phys. Chem. B* **109**, 12663–12676 (2005).
147. S. J. Green and co-workers, *J. Phys. Chem. B* **101**, 2663–2668 (1997).
148. D. I. Gittins and co-workers, *Nature* **408**, 67–69 (2000).
149. Y.-C. Lu and co-workers, *J. Am. Chem. Soc.* **132**, 12170–12171 (2010).
150. Y. Fan and co-workers, *Biosens. Bioelectron.* **26**, 1908–1912 (2011).
151. E. Boisselier and D. Astruc, *Chem. Soc. Rev.* **38**, 1759–1782 (2009).
152. C. M. Goodman and co-workers, *Bioconjugate Chem.* **15**, 897–900 (2004).
153. Y. Pan and co-workers, *Small* **3**, 1941–1949 (2007).
154. H. Takahashi and co-workers, *Langmuir* **22**, 2–5 (2006).
155. T. B. Huff and co-workers, *Langmuir* **23**, 1596–1599 (2007).
156. T. S. Hauck, A. A. Ghazani, and W. C. W. Chan, *Small* **4**, 153–159 (2008).
157. A. P. Demchenko, M. A. H. Muhammed, and T. Pradeep *Luminescent Quantum Clusters of Gold as Bio-Labels*, Springer, Berlin, Germany, 2010.
158. J. Zheng, P. R. Nicovich, and R. M. Dickson, *Annu. Rev. Phys. Chem.* **58**, 409–431 (2007).
159. M. A. Habeeb Muhammed and co-workers, *Chem. Eur. J.* **16**, 10103–10112 (2010).
160. E. S. Shibu and T. Pradeep, *Chem. Mater.* **23**, 989–999 (2011).
161. M. A. Habeeb Muhammed and T. Pradeep, *Small* **7**, 204–208 (2011).
162. M. A. Habeeb Muhammed and co-workers, *Nano Res.* **1**, 333–340 (2008).
163. E. S. Shibu and co-workers, *J. Phys. Chem. C* **112**, 12168–12176 (2008).
164. M. A. Habeeb Muhammed and co-workers, *J. Phys. Chem. C* **112**, 14324–14330 (2008).

165. P. L. Xavier and co-workers, *Nanoscale* **2**, 2769–2776 (2010).
166. M. A. Habeeb Muhammed and co-workers, *Chem. Eur. J.* **15**, 10110–10120 (2009).
167. C. Zhou and co-workers, *Angew. Chem., Int. Ed.* **50**, 3168–3172 (2011).
168. C.-C. Huang and co-workers, *Angew. Chem.* **119**, 6948–6952 (2007).
169. L. D. Socaciu and co-workers, *J. Am. Chem. Soc.* **125**, 10437–10445 (2003).
170. B. Yoon and co-workers, *Science* **307**, 403–407 (2005).
171. H. Häkkinen and co-workers, *Angew. Chem., Int. Ed.* **42**, 1297–1300 (2003).
172. A. Sanchez and co-workers, *J. Phys. Chem. A* **103**, 9573–9578 (1999).
173. S. K. Libutti and co-workers, *Clin. Cancer Res.* **16**, 6139–6149 (2010).

P. R. Sajanlal
T. Pradeep
Indian Institute of Technology Madras